JOURNAL OF MATERIALS SCIENCE 28 (1993) 5931–5936

Static fatigue in ceramic materials: influences of an intergranular glassy phase and fracture toughness

GUEN CHOI
National Research Institute for Metals, Tsukuba Laboratories, 1-2-1, Sengen, Tsukuba City, Ibaraki 305, Japan

SUSUMU HORIBE
Department of Materials Science and Engineering, Waseda University, 3-4-1, Ohkubo, Shinjuku, Tokyo 169, Japan

Static fatigue behaviour in various kinds of non-transforming ceramics has been investigated. It was found that static fatigue is closely related to the presence of a glassy phase between adjacent grains, as well as fracture toughness. Non-oxide ceramics, such as reaction-bonded silicon nitride which scarcely contains the glassy phase (group I), are insensitive to static fatigue, whereas non-transformation oxide ceramics, like alumina and non-oxide ceramics such as silicon nitride which contains the glassy phase (group II), are sensitive to static fatigue. However, static fatigue behaviour in the materials of group II also depends strongly on fracture toughness. K_{IC}. Namely, fatigue parameter n increases linearly as K_{IC} increases. From such a dependence the life time relation in the materials of group II is proposed as $t_s = B\sigma_s^{-CK_{IC}}$ in terms of applied stress σ_s and K_{IC}.

1. Introduction

It is well known that ceramic materials are subjected to subcritical crack growth by a mechanism involving environmentally assisted cracking processes under sustained loading. One refers to this phenomenon as static fatigue. Although static fatigue in ceramics has been investigated widely [1–4], details of the mechanism are still uncertain. It is important to understand the mechanism for the application of ceramics to structural components.

Static fatigue in glass is due to reaction with water in air, especially at crack-tip locations where glass is highly stressed. The ensuing chemical reaction can be written as [5]

$$H_2O \text{ (atmosphere)} \rightarrow H_2O \text{ (in glass)} \quad (1)$$

$$H_2O \text{ (in glass)} + [\text{Si–O–Si}] \rightarrow 2[\text{SiOH}] \quad (2)$$

This reaction leads to a break in the Si–O bond in the glass. The attendant reaction with the water molecule proceeds as per Equation 2. It has been supposed that similar reactions are also able to occur for non-oxide ceramics. Yamauchi *et al.* [6] have reported that static fatigue in non-oxide ceramics depends on the amount of intergranular glassy phase due to oxide additives and its effect is enhanced with an increase in the amount of the glassy phase. This implies that static fatigue may be governed by a reaction associated not with the matrix but with the glassy phase. For dense silicon nitride and silicon carbide having the glassy phase, the path of slow crack growth is along the grain boundary, whereas it is intragranular for ceramics without the glassy phase [7]. It is thus expected that the former are susceptible to static fatigue, since the glassy phase is located at the grain boundary alone.

Toughening is generally explained by a crack tip shielding mechanism, such as crack deflection, grain bridging, microcracking and phase transformation. If static fatigue is related to toughness alone, highly toughened materials are insensitive to static fatigue, because of a reduction in stress at the crack tip due to crack tip shielding. It is well known that fracture toughness is seriously affected by microstructural changes. The relation between microstructures and fracture toughness has been relatively well investigated for silicon nitride. For example, an increase in the aspect ratio leads to a linear increase in fracture toughness, and an increase in grain size with comparable grain morphology also causes fracture toughness to increase. These factors are dependent upon powder properties (type and phase composition of the starting powders, impurity content), type and amount of sintering additives and processing parameters (time, temperature, pressure) [9–14].

Toughening of ceramics like silicon nitride has been practically achieved by addition of a proper amount of oxide additives such as MgO, Y_2O_3 and Al_2O_3. If it is related to the presence of the glassy phase, as well as fracture toughness, static fatigue behaviour in ceramic materials toughened in such a way is not easily predicted, because static fatigue may be not only restrained by crack tip shielding, but also enhanced, due to the feasibility of chemical reaction with the glassy phase located at the grain boundary. In order to

0022–2461

understand static fatigue behaviour in such materials, we should consider the influence of factors such as presence of the glassy phase, microstructure and fracture toughness.

In this study we have investigated the influence of such factors on static fatigue, using various kinds of ceramic materials. On the basis of the experimental results obtained and other data available, static fatigue behaviour is discussed.

2. Experimental procedure

2.1. Materials

Various kinds of ceramic materials, such as silicon nitride, sialon, silicon carbide and alumina, were prepared for the present experiment. The processing conditions of the materials used are shown in Table I. Material SSN-1 was normally sintered at 1750 °C with Y_2O_3–$MgAl_2O_4$ additives. SSN-2 was fabricated under the identical conditions as SSN-1, except for variation of contents of additives. Contents of additives were varied to obtain rod-like β-phase grain morphologies with very different aspect ratios. According to the study of Wotting and Ziegler [12] for silicon nitride containing Al_2O_3–Y_2O_3 as additives, an increase in the amount of Al_2O_3 leads to a decrease in fracture toughness, due to a reduction in the aspect ratio, whereas fracture toughness increases with increasing Y_2O_3, resulting in an increase in the aspect ratio. On the basis of this result, SSN-1 of high Y_2O_3 content and low Al_2O_3 content, and SSN-2 of high Al_2O_3 content and low Y_2O_3 content were selected for this study. It is thus expected that the aspect ratio is higher in SSN-1 than in SSN-2. Material RBSN was reaction-bonded at 1450 °C and consisted of a mixture of α and β phase crystals.

Aluminas with equiaxial grain morphologies were sintered using the same high purity alumina powder (99.995%) without additives and subsequent HIP processing. Variation of grain size is obtained by changing HIP processing temperature. ALO-1 was produced by HIP processing at 1700 °C, whereas ALO-2 was made by HIP processing at 1400 °C.

α-sialon ceramics are formed by the reaction as follows

$$a\,Si_3N_4 + b(9AlN + Y_2O_3) \rightarrow cY_x(Si, Al)_{12}(O, N)_{16} \quad (3)$$

where x varies from zero to 0.8 at 1750 °C. For $0 < x < 0.3$, (α + β) sialon, which consists of a mixture of β-Si_3N_4 and α-sialon, is obtained, whereas for $0.3 \leqq x \leqq 0.8$, α-sialon alone is obtained [15]. In this study, x-values are 0.2 for SA-1 of (α + β)-sialon and 0.5 for SA-2 of α-sialon.

TABLE I Processing conditions of materials used

Materials		Additives	Processing method	Phase
Si_3N_4	SSN-1	$Y_2O_3 + Al_2O_3$	Sintered	β
	SSN-2	$Y_2O_3 + Al_2O_3$	Sintered	β
	RBSN		Reaction bonded	α + β
Al_2O_3	ALO-1		HIP	α
	ALO-2		HIP	α
Sialon	SA-1	Y_2O_3 + AlN	Sintered	α + β
	SA-2	Y_2O_3 + AlN	Sintered	α

2.2. Static fatigue test

These materials, with dimensions of about 4 × 5 × 45 mm, were ground and lapping polished to produce the specimens for the fatigue test, with dimensions of 3 × 4 × 40 mm. Before fatigue testing, two or three precracks were introduced at the centre of the specimen by a Vickers indentor, using loads of 98 N for silicon nitrides and 49 N for the remainder.

Fatigue tests using the specimens with two or three precracks provide conservative data for the fatigue lives of materials, compared with tests of specimens with a single crack [16]. Different indentation loads were employed to keep the precrack size almost the same, irrespective of the kinds of materials. Precrack size of specimens was 200–300 μm, except for reaction-bonded silicon nitride. Since indentation load for RBSN was selected to lead to a larger precrack size than pore size, the precrack size in RBSN is larger than that in other materials.

Static fatigue tests were conducted in four point bending (outer span 30 mm, inner span 10 mm), using an electrohydraulic testing system. All experiments were carried out at room temperature in air.

3. Results

3.1. Microstructures and fracture toughness

Figs 1 and 2 show scanning electron micrographs of the fracture surface of silicon nitride and sialon ceramics, respectively. From these figures it is indicated that all these materials have rod-like structures and also fracture intergranularly. For silicon nitride ceramics both aspect ratio and grain size are a few times larger in SSN-1 than in SSN-2.

For sialon ceramics grain size is coarser in α-sialon than in (α + β)-sialon, whereas aspect ratio is larger in the latter than in the former.

Table II shows fracture toughness, grain size and morphology of the materials used in this study. SSN-1 with a high aspect ratio and coarse grains shows a higher fracture toughness, as compared with SSN-2 of low aspect ratio and fine grains. Such a tendency is in agreement with results by Wotting and Ziegler [12]. RBSN shows very low fracture toughness. Generally, it has been reported that reaction-bonded silicon nitride ceramics are poor in toughness, although they have rod-like structures [13, 16]. It is thought that this is due to a high pore density and not containing a glassy phase at the grain boundary [13, 17].

On the other hand, SA-1 of (α + β)-sialon with fine grains shows a higher K_{IC} than SA-2 of α-sialon with coarse grains. This may be attributed to the higher aspect ratio of SA-1. However, K_{IC} of SA-1 is lower than that of SSN-1, though they have almost the same aspect ratio. From these results it is understandable that fracture toughness depends on grain size, as well as aspect ratio.

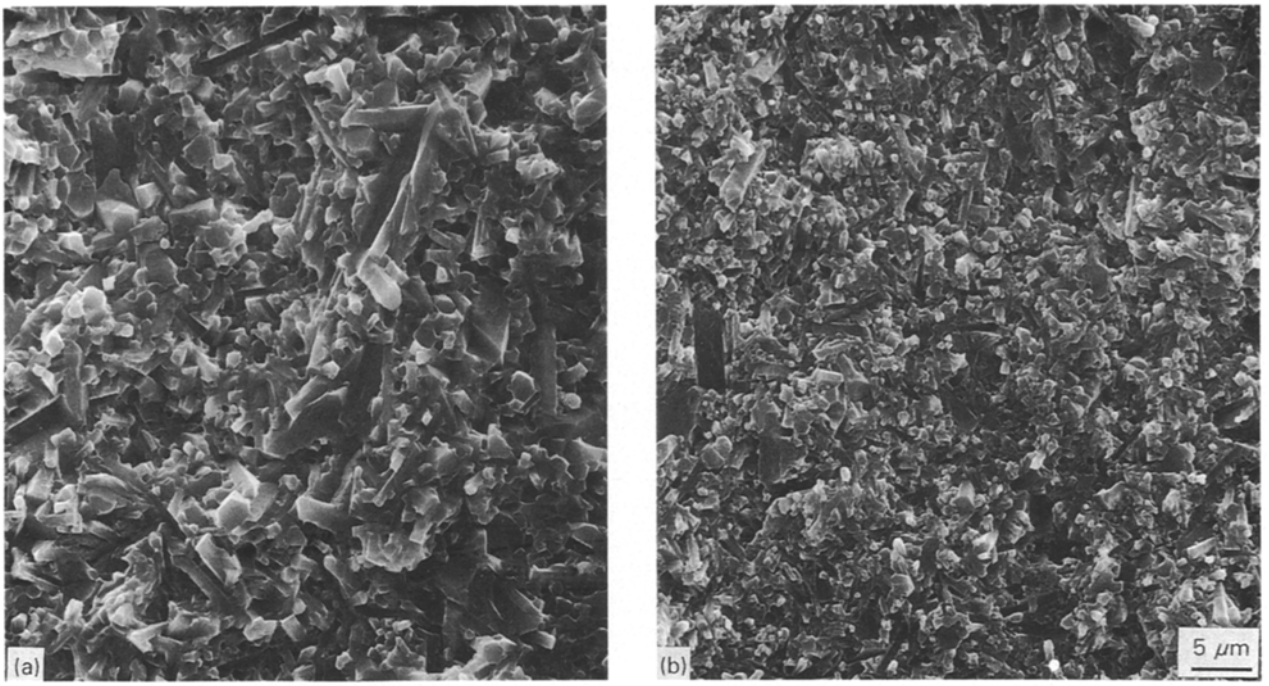

Figure 1 Scanning electron micrographs of fracture surfaces of silicon nitride ceramic materials: (a) SSN-1; (b) SSN-2.

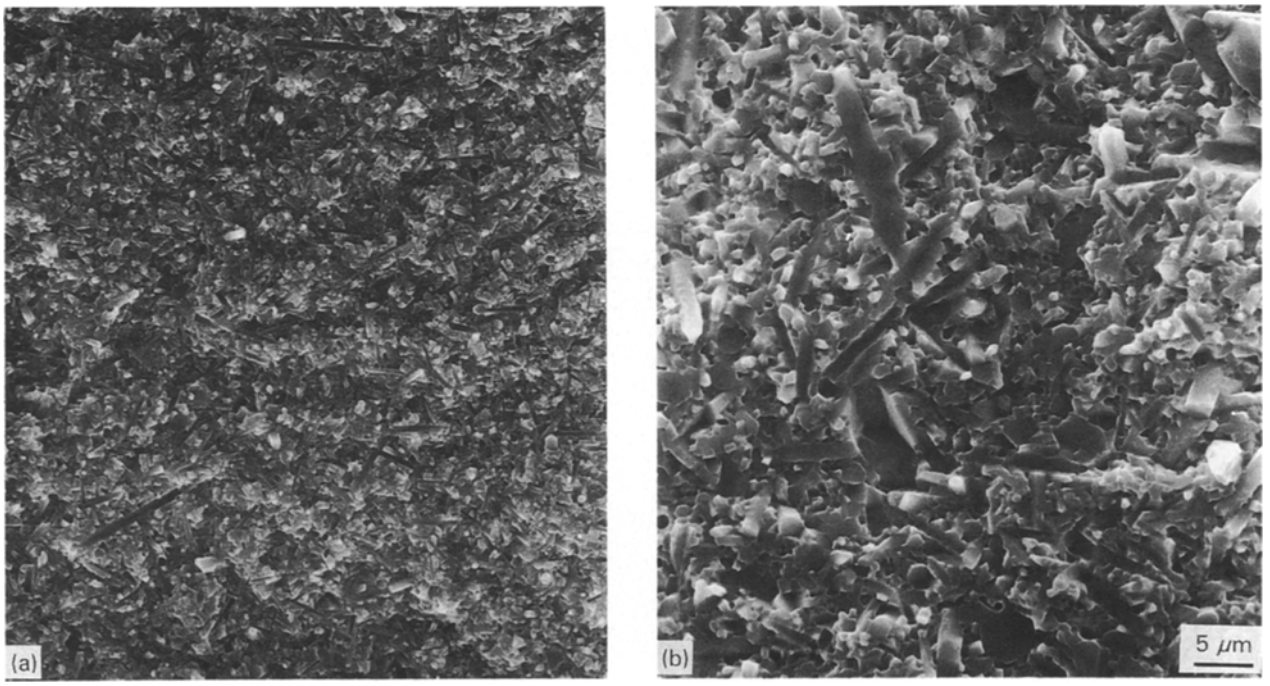

Figure 2 Scanning electron micrographs of fracture surfaces of sialon ceramic materials: (a) SA-1; (b) SA-2.

In the case of alumina with equiaxed grain structure, fracture toughness also increases with increasing grain size. However, the toughness in alumina is considerably lower than that in silicon nitride, although the grain size of alumina is a few times as large as that of silicon nitride. It is likely that such a difference in toughness is attributed to the effect of grain morphology, because the value of toughness of silicon nitride having equiaxed grain morphologies is about 3 MPa $m^{1/2}$, almost equal to that of alumina [10].

3.2. Static fatigue behaviour

For most ceramic materials the rate of crack growth under static load is generally expressed by the simple power law:

$$\frac{da}{dt} = AK_I^n \tag{4}$$

where a is the crack size, t is time, A and n are constants, and K_I is the stress intensity factor. K_I is given by:

$$K_I = Y\sigma_s a^{1/2} \tag{5}$$

TABLE II Mechanical and microstructural properties of materials used

Materials		Flexural stress (MPa)	K_{IC} (MPam$^{1/2}$)	Grain size (μm)	Morphology
Si_3N_4	SSN-1	669	6.5	1.0	Rod-like
	SSN-2	764	5.0	0.5	Rod-like
	RBSN		2.5		Equiaxial
Al_2O_3	ALO-1	670	3.1	10	Equiaxial
	ALO-2	438	2.5	2.0	Equiaxial
Sialon	SA-1	1039	5.5	0.3	Rod-like
	SA-2	676	4.4	1.0	Rod-like

where Y is a geometric factor and σ_s is the applied stress. According to the K-concept of fracture mechanics, failure occurs when K_I reaches a critical value, K_{IC}. For static bending tests with σ_s the lifetime, t_f, can be calculated by integration of Equation 4 to yield [18]:

$$t_f = B\sigma_s^{-n}, \quad B = \frac{2\sigma_c^{n-2}}{A(n-2)Y^2K_{IC}^{2-n}} \qquad (6)$$

where σ_c is the inert strength, i.e. the strength in the absence of subcritical crack extention.

Fig. 3 shows static fatigue lives, t_f, as a function of the applied stress, σ_s, for various silicon nitrides with different microstructure: SSN-1, SSN-2 and RBSN. Scatter in these data was very small, compared with preceding results [19]. It is indicated in this figure that there are linear decreases in stress and subsequent plateaux at lower stresses for all materials, though there is a difference in their slope. Such tendencies are also observed in other ceramics, as shown in Figs 4 and 5. These results indicate that static fatigue behaviour can be well expressed by Equation 6. Static fatigue degradation is very small in SSN-1 and RBSN, whereas it is prominent in SSN-2.

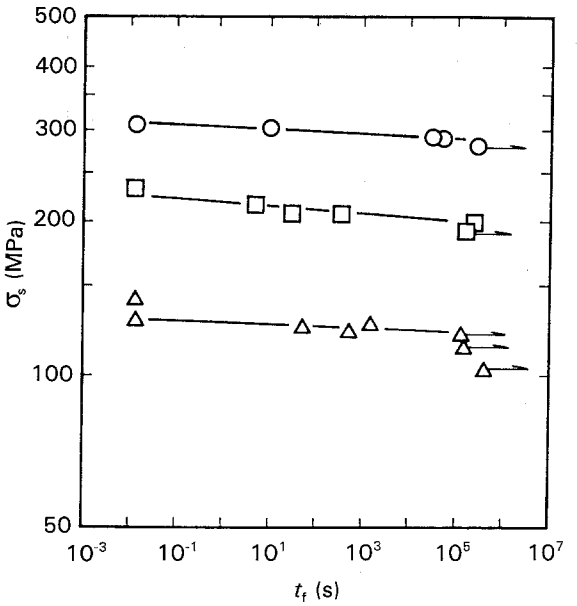

Figure 3 Static fatigue lifetimes for various kinds of silicon nitride materials. (○) SSN-1; (□) SSN-2; (△) RBSN.

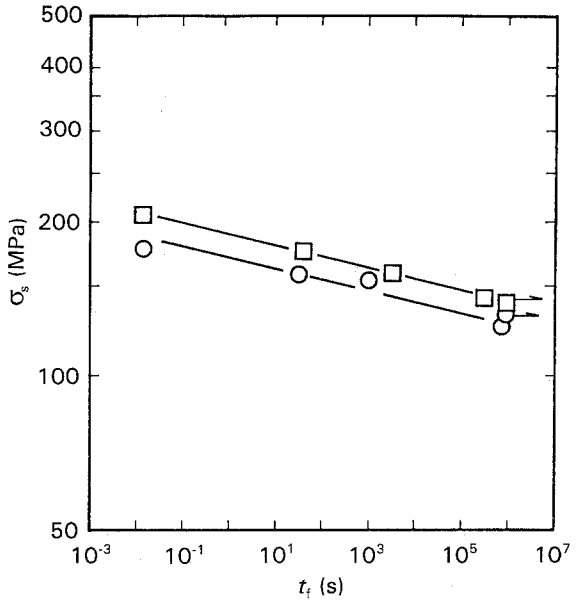

Figure 4 Static fatigue lifetimes for aluminas with two different grain sizes: (□) ALO-1; (○) ALO-2.

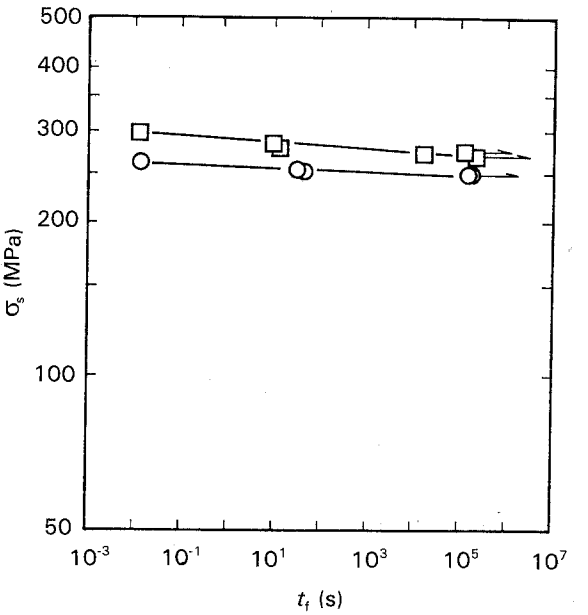

Figure 5 Static fatigue lifetimes in SA-1 of (α + β)-sialon and SA-2 of α-sialon: (□) SA-1; (○) SA-2.

Fig. 4 shows static fatigue lifetimes in aluminas with different grain size [20]. From this figure it is understandable that static fatigue degradation is not affected by grain size. In addition, the degradation in alumina is considerably larger than that in silicon nitride.

Fig. 5 shows static fatigue lifetimes in sialon ceramics. This figure shows that α-sialon is hardly subject to static fatigue effects.

4. Discussion

4.1. Influence of the presence of a grain boundary glassy phase

It has been known that static fatigue in ceramics is responsible for stress corrosion cracking, related to

TABLE III Oxygen contents of non-oxide ceramic materials used

Materials		O (wt %)
Si_3N_4	SN-1	4.8
	SSN-2	5.8
	RBSN	1.8
Sialon	SA-1	2.4
	SA-2	3.8

water in air. Yamauchi et al. [6] have investigated the dynamic fatigue behaviour of various kinds of ceramics and shown that static fatigue resistance in non-oxide ceramics decreases with an increase in the amount of intergranular glassy phase, without regard to the kinds of ceramics. This result implies that stress corrosion cracking is related not to the matrix itself, but to interfaces between matrix and glassy phase at the grain boundary or to glassy phase at the grain boundary, because cracks in ceramics with the glassy phase grow intergranularly. Besides, it is well known that α-sialon and reaction-bonded silicon nitride scarcely have an intergranular glassy phase [13, 21]. Therefore, the fact that such materials are insensitive to static fatigue can be explained by the suggestion of Yamauchi and coworkers [6].

However, the results for silicon nitride ceramics and (α + β)-sialon with the glassy phase are inexplicable by their suggestion alone. Because although (α + β)-sialon has a lower oxygen content than SSN-1, as shown in Table III, the former is more sensitive than the latter to static fatigue. Furthermore, static fatigue degradation is substantially smaller in SSN-1 than in SSN-2, in spite of these materials having almost the same oxygen contents. Therefore, it is thought that static fatigue behaviour in these materials is associated with other factors, besides the amount of intergranular glassy phase.

4.2. The influence of fracture toughness

Some researchers [22, 23] have reported that static fatigue depends upon the microstructure of the ceramic materials tested. As noted in Section 3, microstructures are closely related to fracture toughness. Hence, it is expected that static fatigue depends on fracture toughness. In ceramic materials toughening has been explained in general by the mechanisms of crack tip shielding. These mechanisms are expressed as [8].

$$K_{tip} = K_{I\max} - K_s \quad (7)$$

where K_{tip} is the stres intensity factor at the crack tip, $K_{I\max}$ the maximum stress intensity factor, and K_s the stress intensity factor due to shielding. From Equations 4 and 7 it is expected that static fatigue lifetimes in a ceramic material increase with an increase in fracture toughness, because of a reduction of stress at the crack tip by crack tip shielding. As shown in Figs 3–5, lifetimes in the same kind of ceramics increase with an increase in fracture toughness.

However, in order to predict quantitatively static fatigue lifetimes, the n value, which indicates the degree of static fatigue resistance of a material, should be determined. So far, n value is only known as a constant value depending on material. Fig. 6 shows the relationship between the applied stress normalized by flexural stress and time to failure for alumina and non-oxide ceramics which involve a glassy phase. From this figure it is recognized that static fatigue degradation in these materials is enhanced as fracture toughness increases, without regard to the kinds of material.

Static fatigue degradation in aluminas is large, in spite of scarcely containing an intergranular glassy phase. Kawakubo *et al.* [19] have shown that oxide ceramics such as alumina are sensitive to static fatigue and the degree of static fatigue degradation is almost the same as with glass. According to Himsolt *et al.* [10] and Faber *et al.* [24], the K_{IC} of equiaxed grained silicon nitride is smaller than half of the K_{IC} of rod-like grained silicon nitride, and almost equal to the K_{IC} of aluminas. Moreover, static fatigue degradation in silicon nitride is remarkably larger in the former than in the latter. Therefore, it is thought that low fracture toughness and large static fatigue degradation in alumina is attributed to its equiaxed structure.

Himsolt *et al.* [10] have investigated subcritical crack growth behaviour of hot pressed silicon nitride ceramics with different grain structures and shown that as K_{IC} increases, crack growth rate is restrained and also the n value rises. This implies that the value of n depends upon K_{IC} in some way.

The relation between K_{IC} and n for the materials used in this study is shown in Fig. 7. As shown in this figure, the materials are divided into two groups: a non-glassy phase group (group I) of which the n value is independent of K_{IC}, and an oxide or glassy phase group (group II) whose n value depends on K_{IC}. It is expected that silicon carbide (additives: B, C) having no grain boundary phase belongs to group I. On the other hand, the n value of materials of group II

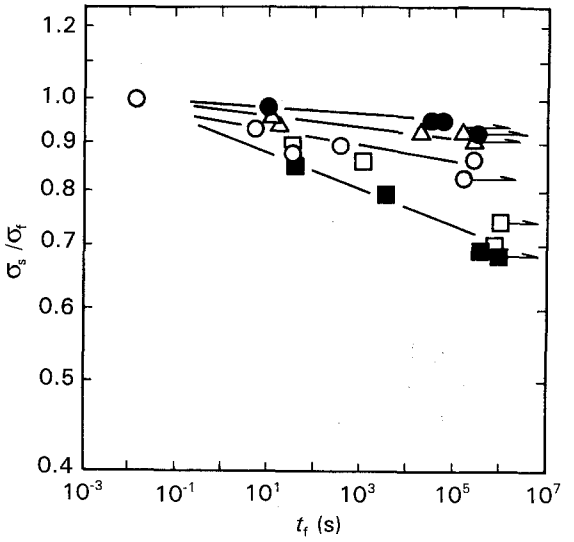

Figure 6 Comparison of static fatigue lifetimes in various kinds of ceramic materials plotted as a function of the normalized applied stress: (●) SSN-1; (○) SSN-2; (■) ALO-1; (□) ALO-2; (△) SA-1.

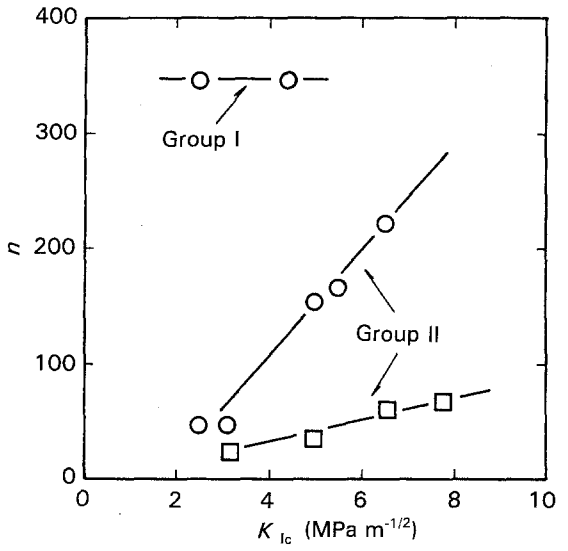

Figure 7 The relation between n and K_{IC}, containing the data for silicon nitride ceramic materials of Himsolt *et al.* [10]: ○ present work; □ Himsolt *et al.*

increases linearly with increasing K_{IC}, without regard to the kinds of material. Such a relation is also obtained by replotting the data of Himsolt and Knoch [10]. Therefore, the relation between n and K_{IC} for materials of group II can be expressed as follows

$$n = CK_{IC} \quad (8)$$

where C is constant. However, as shown in Fig. 7, a considerable difference in the slope between the present work and previous work is shown. It is thought that this is in part attributed to a difference in precrack size, because of the use of a long crack in previous work. In fact, it has been reported that static fatigue degradation in silicon nitride increases as precrack size increases [25]. From Equation 8, Equations 4 or 6 are given as follows

$$\frac{da}{dt} = AK_I^{CK_{IC}}$$

or

$$t_s = B\sigma_s^{-CK_{IC}} \quad (9)$$

Therefore, it is concluded that for non-oxide ceramics which involve a glassy phase and oxide ceramics such as alumina, static fatigue behaviour is related closely to fracture toughness, K_{IC}, i.e. static fatigue is considerably restrained by an increase in K_{IC}, resulting in a decrease in stress in the crack tip as well as an increase in the value of n.

5. Conclusions

Static fatigue behavior was investigated for various kinds of non-transforming ceramics. The main results obtained are as follows:

(i) Static fatigue depends on the presence of an intergranular grassy phase. Non-oxide ceramics, such as RBSN and α-sialon, which scarcely contain an intergranular glassy phase, are insensitive to static fatigue. In contrast, non-transforming oxide ceramics like alumina, as well as non-oxide ceramics such as silicon nitride and (α + β)-sialon, which contain the glassy phase, are sensitive to static fatigue.

(ii) Static fatigue behaviour in oxides or materials containing a glassy phase also depends strongly upon K_{IC}. Namely, static fatigue degradation is considerably restrained by an increase in K_{IC}, which results in a decrease of stress at the crack tip as well as a linear increase in the n value with increasing K_{IC}.

(iii) From this result, the modified lifetime relation is suggested as $t_s = B\sigma_s^{-CK}$.

References

1. J. E. RITTER and J. N. HUMENIK, *J. Mater. Sci.* **14** (1979) 626.
2. S. M. WIEDERHORN, S. W. FREIMAN, E. R. FULLER and C. J. SIMMONS, *ibid.* **17** (1982) 3460.
3. P. F. BEACHER, *J. Amer. Ceram. Soc.* **66** (1983) 485.
4. T. A. MICHALSKE, B. C. BUNKER and S. W. FREIMAN, *ibid.* **69** (1986) 721.
5. S. W. FREIMAN, in "Strength of inorganic glass", edited by C. R. Kurjian (Plenum Press, New York, 1985) p. 197.
6. Y. YAMAUCHI, S. SAKAI, M. ITO, T. OHJI, W. KANEMATSU and S. ITO, *J. Ceram. Soc. Jpn* **96** (1988) 885.
7. S. HORIBE and R. HIRAHARA, *Acta Metall. Mater.* **39** (1991) 1309.
8. R. O. RITCHIE, *Mater. Sci. Engng* **A103** (1988) 15.
9. F. F. LANGE, *J. Amer. Ceram. Soc.* **64** (1976) 371.
10. G. HIMSOLT and H. KNOCH, *ibid.* **62** (1979) 29.
11. R. W. RICE, S. W. FREIMAN and P. F. BECHER, *ibid.* **64** (1981) 345.
12. G. WÖTTING and G. ZIEGLER, *Ceram. Int.* **10** (1984) 18.
13. G. ZIEGLER, J. HEINRICH and G. WÖTTING, *J. Mater. Sci.* **22** (1987) 3041.
14. E. M. KNUTSON-WEDEL, L. K. L. FALK, H. BJORKLUND and T. EKSTROM, *ibid.* **26** (1991) 5575.
15. K. ISHIZAWA, N. AYUZAWA, H. HAISHI, A. SHIRANITA, M. TAKAI and M. MITOMO, in "Silicon nitride ceramics", Vol. 2, edited by S. Somiya and Y. Inomata (Uchida Rokakuho, Tokyo, Japan, 1990) p. 239.
16. S. HORIBE, *J. Eur. Ceram. Soc.* **6** (1990) 89.
17. K. KISHI, S. UMEBAYASHI and E. TANI, *J. Mater. Sci.* **25** (1990) 2780.
18. J. E. RITTER Jr, in "Fracture mechanics of ceramics", Vol. 4, edited by R. C. Bradt, D. P. H. Hasselman and F. F. Lange (Plenum, New York, USA, 1978) p. 667.
19. T. KAWAKUBO, N. OKABE and T. MORI, in "Fatigue '90", Vol. 2, edited by H. Kitagawa and T. Tanaka (Mat. Comp. Eng. Publ., Ltd., Edgbaston, UK, 1990) p. 745.
20. S. HORIBE and E. TAKAKURA, *Ann. Chim. Fr.* **16** (1991) 403.
21. T. EKSTROM and M. NYGREM, *J. Amer. Ceram. Soc.* **75** (1992) 259.
22. J. E. RITTER Jr and M. S. CAVANAUGH, *ibid.* **57** (1974) 480.
23. B. J. PLETKA and S. M. WIEDERHORN, *J. Mater. Sci.* **17** (1982) 1247.
24. K. T. FABER and A. G. EVANS, *Acta Metall. Mater.* **31** (1983) 577.
25. A. UENO, H. KISHIMOTO and H. KAWAMOTO, *J. Soc. Mater. Sci. Jpn* **41** (1992) 495.

Received 20 October 1992
and accepted 1 March 1993